Hyaluronic Acid-decorated PLGA-PEG Nanoparticles for Targeted Delivery of SN-38 to Ovarian Cancer

KIRAN KUMAR VANGARA[1], JINGBO LOUISE LIU[2] and SRINATH PALAKURTHI[1]

[1]*Department of Pharmaceutical Sciences, Irma Lerma Rangel College of Pharmacy, Texas A&M Health Science Center, Kingsville, TX, U.S.A.;*
[2]*Department of Chemistry, Texas A&M University-Kingsville, Kingsville, TX, U.S.A.*

Abstract. *Background: Extreme hydrophobicity and poor stability of SN-38, a highly potent topoisomerase I inhibitor, has prevented its clinical use. Its encapsulation into nanoparticles may be a way to overcome these problems. Here we report the use of SN-38-loaded hyaluronic acid (HA)-decorated poly(lactic-co-glycolic acid)-polyethylene glycol (PLGA-PEG) nanoparticles (NPs) for targeted ovarian cancer therapy. Materials and Methods: PLGA-PEG nanoparticles loaded with SN-38 were prepared by single- emulsion (O/W) solvent evaporation method. HA was decorated onto the nanoparticles by 1-ethyl-3-(3-dimethylaminopropyl)carbodiimide (EDC) coupling and the extent of HA conjugation was quantified by hexadecyltrimmethylammonium bromide (CTAB) assay. Cancer cell specificity of the NPs was determined by flow cytometry and cytotoxicity of the NPs was tested by 3-[4,5-dimethylthiazol-2-yl]-2,5-diphenyl tetrazolium (MTT) bromide assay. Results: Mean size, zeta potential and encapsulation efficiency of PLGA-PEG-HA NPs were 265.6±3.8 nm, -30.4±0.1 mV and 75.8±4.1%, respectively. Cellular uptake of PLGA-PEG-HA NPs was 8- and 16-fold higher in CD44-positive cell lines, SKOV-3 and OVCAR-8, as compared to CD44-negative cells (CHO). Cytotoxicity of the targeted NPs was significantly higher as compared to non-targeted NPs for the above cell lines. These results suggest that PLGA-PEG-HA NPs could be an efficient delivery system for SN-38 for targeted therapy of ovarian cancer.*

Correspondence to: Srinath Palakurthi, Ph.D., Associate Professor, Irma Lerma Rangel College of Pharmacy, Texas A&M Health Science Center, Kingsville, TX, U.S.A. Tel: +1 3612210748, Fax: +1 3612210793, e-mail: palakurthi@tamhsc.edu

Key Words: CD44-targeted delivery, PLGA nanoparticles, hyaluronic acid, surface decoration, SN-38, ovarian cancer, CTAB assay.

Ovarian cancer is the leading cause of gynecological cancer mortality and is the fifth leading cause of cancer deaths among American women (1). According to American Cancer Society statistics for the year 2013, the number of ovarian cancer cases diagnosed will be about 22,240 and about 14,030 women will die from the same (2). Early detection and treatment can increase the five-year survival rate to >92%. Unfortunately most patients are diagnosed at advanced stages with disseminated tumor cells in the peritoneal cavity and only approximately 50% of women survive longer than five years after diagnosis. Primary treatment of ovarian cancer involves surgical removal of ovaries followed by chemotherapy or radiation therapy. The majority of the patients experience frequent disease relapse in about two years and generally do not respond to chemotherapy due to development of chemoresistance (3). Targeted delivery of high doses of chemotherapeutics using cancer-specific ligands is an attractive alternative to treat metastatic and resistant tumors (4-6). One such important ligand explored in recent years is hyaluronic acid (HA), which has high affinity and specificity for CD44 receptors (7, 8).

For a decade, CD44 has been recognized as the most promising cell surface biomarker for metastatic cancer (9) and cancer stem cells (10, 11). CD44 receptors are overexpressed in many cancer types and play an important role in tumor progression, being involved in metastasis, invasion, adhesion and angiogenesis (7). HA, which is the primary ligand for CD44 receptors, has been investigated for targeted drug delivery for many types of cancers including of the head and neck, breast, stomach, ovarian, colorectal, lung, liver, pancreas, and bladder (8, 12, 13). HA is a natural linear polysaccharide present in extracellular matrix, and plays an important role in cell proliferation, differentiation, motility, adhesion and gene expression. HA can be efficiently taken up by cells through CD44 receptor-mediated endocytosis. Because of its specificity towards cancer cells and its bio-inertness, HA has been used as drug carrier, and ligand on various nanoparticles (14, 15). HA

targeted drug delivery (14, 15) and gene delivery (16) systems showed excellent targetability in *in vitro* and murine tumor models.

Polymeric nanoparticles offer great advantage by delivering higher concentration of chemotherapeutics to tumor site and thus reducing unwanted systemic toxic effects. Among polymeric nanoparticles, poly(lactic-*co*-glycolic acid) (PLGA) nanoparticles have received great attention due to their biocompatible and biodegradable properties. PLGA has been approved by the Food and Drug Administration (FDA) and European Medical Agency (EMA) in drug delivery systems for parenteral administration. PLGA nanoparticles have been successfully used for passive tumor targeting by EPR effect or active targeting by offering good possibility to modify its surface with tumor-specific ligands. However, PLGA nanoparticles with a targeting moiety have shown better activity in preclinical studies in comparison to their non-targeted nanoparticles (17). Only two reports on PLGA nanoparticles with HA as targeting moiety have been reported, for delivery of doxorubicin (18) and 5-fluorouracil (19).

SN-38 (7-ethyl-10-hydroxy-camptothecin) is an active metabolite of irinotecan. It is about 100- to 1000-fold more potent than irinotecan and acts by inhibiting topoisomerase I. Only 2-8% of irinotecan is converted to its active form SN-38 in liver and cancer cells, and therefore a high dose of irinotecan needs to be administered to get the desired therapeutic effect. Clinical use of SN-38 is limited by its poor aqueous solubility and instability at physiological pH. The water solubility of SN-38 is 7.2 μg/ml and the lactone ring of SN-38 converts to its pharmacologically-inactive carboxylate form at pH >6 (20). To address these solubility and stability issues, incorporation into nanoparticles is reported as one of the best methods (21-23). In pre-clinical studies, liposomal formulation of SN-38 showed increased cytotoxicity in various cancer cell lines and *in vivo* (22). Although a lipid-based nanoparticle formulation has been developed by Ethypharma lnc., PLGA-HA nanoparticles of SN-38 have not been reported thus far (23). Herein we report on HA-decorated PLGA-PEG nanoparticles, their physicochemical characterization, targeting efficacy, mechanism of internalization and cytotoxicity towards ovarian cancer cell lines.

Materials and Methods

Chemicals. PLGA (average M_w 33 kDa) was purchased from Lakeshore biomaterials, Birmingham, AL, USA. HA (average M_w 16.9 kDa) was obtained from Lifecore Biomedical (Chaska, MN, USA) and used after de-salting by dialysis against deionized water. SN-38 was purchased from AK Scientific, Union City, CA, USA. *N,N'*-Dicyclohexylcarbodiimide (DCC), 1-ethyl-3-(3-dimethylaminopropyl) carbodiimide (EDC) and *N*-hydroxysuccinimide (NHS) were purchased from Thermo Scientific, Rockford, IL, USA. Polyethylene glycol *bis* amine (PEG *bis* amine, M_w 2000 Da), poly vinyl alcohol (M_w 31,000-50,000 g/mol), 3-[4,5-dimethylthiazol-2-yl]-2,5-diphenyl tetrazolium bromide (MTT), fluorescein isothiocyanate (FITC), hexadecyl-trimmethylammonium bromide (CTAB) and colchicine were purchased from Sigma Aldrich, St. Louis, MO, USA.

Cell culture. SKOV-3 (human ovarian carcinoma) and Chinese hamster ovary (CHO) cell lines were obtained from the American Type Culture Collection (ATCC, Manassas, VA, USA) and cultured in Dulbeco's modified Eagle's medium (DMEM) and F12 medium, respectively. OVCAR-8 (human ovarian carcinoma) cells were obtained from the National Cancer Institute (NCI), Bethesda, MD, USA and cultured in RPMI-1640 medium. All the media were supplemented with 10% heat-inactivated fetal bovine serum (FBS) and 1% penicillin-streptomycin solution. Cells were incubated in a CO_2 incubator at 37˚C and 95% relative humidity. All cell lines used were of passage number 20-40.

Preparation of HA decorated Nanoparticles. HA-decorated PLGA nanoparticles were prepared in two steps. Firstly, PLGA was conjugated with PEG *bis* amine. Secondly, HA was conjugated onto PLGA-PEG-NH_2 nanoparticles by EDC coupling.

Synthesis and characterization of PLGA-PEG-NH_2. PLGA-PEG-NH_2 was synthesized as reported elsewhere (24).

Activation of COOH group on PLGA. PLGA dissolved in anhydrous methylene chloride was reacted with DCC and NHS for 24 h at room temperature (RT) under nitrogen atmosphere at a stoichiometric molar ratio of PLGA:DDC:NHS was 1:10:10. By product *N,N'*-dicyclohexylurea was removed by filtering through a 0.45-μm Teflon syringe filter. The filtrate was precipitated and washed with ice cold diethyl ether. The precipitate was vacuum dried to obtain activated PLGA.

Conjugation of PEG bis amine with activated PLGA. Activated PLGA and PEG *bis* amine were dissolved in anhydrous methylene chloride (1:1 molar ratio) and reacted overnight at RT under nitrogen. The reaction mixture was precipitated and washed with cold methanol. The precipitate was then vacuum dried to obtain PLGA-PEG-NH_2. The conjugate was dissolved in $CDCl_3$ to a 5 mg/ml solution and was analyzed by nuclear magnetic spectrophotometer (NMR) (500 MHz Bruker, Billerica, MA, USA).

Nanoparticle preparation. PLGA-PEG-NH_2 nanoparticles were prepared by single-emulsion (O/W) solvent evaporation method. Briefly, 20-60 mg of polymer PLGA-PEG-NH_2 was dissolved in 4 ml of methylene chloride. This organic phase was added to 10 ml of 1% polyvinyl alcohol (PVA) aqueous solution and sonicated at 20 W using a probe sonicator (Barson sonifier 250; Barson Ultrasonics, Danbury, CT, USA) for 4 min at 10 s pulse in an ice bath. Organic solvent was evaporated by stirring at RT overnight. The nanosuspension was then centrifuged at 20,000 ×*g* on a Sorvall RC 6+ centrifuge (Thermo Scientific) for 20 min to separate unloaded material and nanoparticles were washed with deionized water to remove excess of PVA.

FITC- or SN-38-loaded nanoparticles were also prepared by same method: 500 μl of 3 mg/ml FITC solution in acetone was added to the organic phase, whereas in the case of SN-38, solution in dimethyl sulfoxide (DMSO) was added to the organic phase. For loading SN-38 into nanoparticles, the pH of the 1% PVA solution was adjusted to 3.1 with 0.1 N HCl. Unencapsulated FITC or SN-38 was removed by centrifugation followed by passing the

nanoparticles through sephadex™ G-25 column (PD10; GE Healthcare Bio-Sciences Corp, Piscataway, NJ, USA). Nanoparticles were lyophilized with 1% sucrose as cryoprotectant.

Preparation of HA-conjugated nanoparticles. HA was conjugated onto the surface of nanoparticles as reported earlier (25). Briefly, HA was presoaked in pH 4.7 2-(*N*-morpholino)ethanesulfonic acid (MES) buffer overnight for complete solubilization and swelling. –COOH groups of HA were activated by treating with EDC and NHS for 2 h in the same buffer. PLGA-PEG-NH_2 nanoparticles were added to the activated HA and stirred overnight to obtain nanoparticles decorated with HA. Excess of HA was removed by three cycles of centrifugation at 15000 × *g* for 20 min.

CTAB turbidimetric assay. HA conjugation onto nanoparticles was confirmed and quantified by a reported indirect method using a CTAB turbidimetric assay (25). The amount of unconjugated HA in the supernatant after centrifugation was quantified and the amount of conjugated HA was calculated by subtracting the amount in the supernatant fraction from the total amount used in the reaction. Briefly, 50 µl of HA standard solution (0.2-1 mg/ml) or supernatant sample was added in triplicate to a 96-well plate. All the samples were incubated with 50 µl of 0.2 M sodium acetate buffer, pH 5.5 at 37˚C for 10 min. Then 100 µl of 10 mM CTAB solution was added to the wells and the absorbance of the precipitated complex was read within 10 minutes at 570 nm using Novostar microplate reader (BMG Lab Technologies, Cary, NC, USA).

Size and zeta potential. Nanoparticles were measured for their size, polydispersity and zeta potential by dynamic light scattering using ZetaPALS zeta potential analyzer (Brookhaven Instruments Corporation, Holtsville, NY, USA).

Toxicity of PLGA-PEG-HA nanoparticles. Toxicity of PLGA-PEG-HA nanoparticles was evaluated by MTT assay on CHO cells. CHO cells were plated at a density of 10,000 cells per well in a 96 well plate. When cells were 80% confluent, they were treated with PLGA-PEG-HA nanoparticles at a concentration of 1-100 µg/ml and incubated for 8 h at 37˚C. Following the incubation period, all the media were aspirated and 50 µl of 0.5 mg/ml of MTT solution in serum-free media was added. After 4 h of incubation, 150 µl of DMSO was added to each well to dissolve the formazan crystals and plates were incubated for a further 1 h. After thorough mixing of each well, the optical density was measured at 570 nm using a microplate reader. Viability of the cells exposed to nanoparticles was expressed as a percentage of the viability of cells grown in the absence of nanoparticles.

CD44 receptor expression analysis by flow cytometry. BD Biosciences (San Jose, CA, USA) support protocol was followed for the CD44 expression by flow cytometer. Briefly, 0.5×10^6 cells/sample were suspended in 50 µl of cold stock buffer [0.2% bovine serum albumin (BSA) in 1× phosphate buffer saline (PBS)]. Then cell suspension was treated with 10 µl of FITC-labeled CD44 antibody (BD Biosciences) in amber-colored microcentrifuge tube as per supplier's instructions, mixed properly and incubated for 30 min at 4˚C in the dark. Cells were washed three times with cold stock buffer, resuspended in stock buffer and analyzed by flow cytometry (BD Accuri C6 Flow Cytometer; BD Biosciences, San Jose, CA, USA) and receptor expression was measured as percentage of cells exhibiting fluorescence.

Specificity of HA conjugated PLGA nanoparticles. For specificity experiments, FITC was loaded into nanoparticles as described earlier and unencapsulated FITC was removed by size-exclusion chromatography. The FITC-loaded nanoparticles were immediately used for cellular uptake studies. Uptake of the nanoparticles was estimated and compared in $CD44^+$ (SKOV-3, OVCAR-8) and $CD44^-$ (CHO) cell lines. Briefly, 1×10^5 cells/well were plated in a 12-well plate, and after reaching 70-80% confluence, cells were treated with 5 µg/ml and 25 µg/ml (from a stock of 5 mg/ml nanosuspension) of FITC loaded PLGA-PEG and PLGA-PEG-HA nanoparticle suspension in serum-free media separately. After 30 min of incubation, cells were washed three times with cold PBS, trypsinized, washed and suspended in stock buffer and analyzed for the percentage of cells with fluorescence using BD Accuri C6 flow cytometer (BD Biosciences).

Mechanism of cellular internalization. To investigate the internalization mechanism of HA-conjugated nanoparticles, cells were pre- and co-incubated with excess of HA (1 mg/ml) or 20 µM of colchicine before the addition of FITC-loaded HA nanoparticles. The concentration of excess HA was selected based on a previous report (25). To differentiate the physical surface adsorption of the HA-conjugated nanoparticles from internalized nanoparticles, cellular uptake was tested at 4˚C and 37˚C.

SN-38 encapsulation efficiency. Encapsulation efficiency was determined by dissolving a known amount of nanoparticles in DMSO and analyzing SN-38 content on a UV-visible spectrophotometer at 380 nm. The minimum detection limit was 1 µg/ml, with R^2 value of 0.9996, and no interference was observed with PLGA and PEG at 380 nm. The percentage encapsulation efficiency (%EE) was calculated using the following formula (26):

$$\%EE = \frac{\text{(Amount of drug in nanoparticles)}}{\text{(Intial amount of drug used)}} \times 100$$

Assessment of SN-38-loaded nanoparticle stability. Stability of SN-38 in nanoparticles was assessed in PBS pH 7.4 and in FBS. Briefly, freez-dried nanoparticle samples (equivalent to 150 µg/ml of SN-38) were dispersed in 3 ml of PBS or FBS, sonicated to disperse any possible lumps and incubated at RT for three days in dark. Each day after thorough mixing, 1 ml of sample was withdrawn and centrifuged at 20000 ×*g*. Supernatant (0.5 ml) was taken and mixed with an equal quantity of acetonitrile acidified with 0.1 N HCl, mixed well and kept aside for 15-20 minutes before analysis by high performance liquid chromatography (HPLC). Particle size and poly dispersity index of the nanoparticles were tested before centrifugation.

HPLC analysis. All stability samples were analyzed on a reverse-phase HPLC system (Waters, Milford, MA, USA) with a binary pump and dual λ absorbance UV-visible detector. We used an HPLC method that can analyze lactone and carboxylate forms of SN-38 simultaneously, as reported earlier with little modifications (27). The chromatographic separations were achieved using an Atlantis® 5 µM 4.6×250 mm C18 column at RT. An isocratic elution method of 1:1 acetonitrile/25 mM NaH_2PO_4 pH 3.1 buffer at a flow rate of 1 ml/min was used. Absorbance was measured at 265 nm. The concentration of SN-38 from each sample was determined from the peak area observed, based on a calibration curve in the concentration range of 0.2-100 µg/ml ($y=79503x + 3907$, $R^2=1$).

Table I. *Physicochemical characteristics of SN-38-loaded nanoparticles (mean±SD, n=3).*

Nanoparticles	Mean diameter nm	PDI	Avg Zeta potential mV	% Encapsulation efficiency
SN38 PLGA-PEG	249.2±0.14	0.155±0.04	–34.48±0.35	81.85±5.33
SN38 PLGA-PEG-HA	265.6±3.82	0.139±0.04	–30.39±0.14	75.83±4.12

PLGA-PEG: Poly(lactic-*co*-glycolic acid)-polyethylene glycol; PLGA-PEG-HA: Poly(lactic-*co*-glycolic acid)-polyethylene glycol-hyaluronic acid; PDI: polydispersity index.

In vitro cytotoxicity of SN-38-loaded nanoparticles. Cytotoxicity of SN-38-loaded nanoparticles was evaluated on SKOV-3 and OVCAR-8 cell lines using MTT assay. Nanoparticles were dispersed in PBS (pH 7.4) and sonicated for one minute to make a uniform dispersion and suitable dilutions were made in required growth media. As SN-38 is not soluble in water, the stock solution was made in DMSO and suitable dilutions were made in growth media, keeping the final DMSO concentration less than 0.1%. Briefly, 0.6-1×10^4 cells per well were plated in a 96-well pate. After 24 h of incubation, cells were treated with different concentrations (0.5 nM to 10 μM) of SN-38 alone or nanoparticles loaded with equivalent amounts of SN-38 and incubated for 72 h. Cells were then washed with PBS and 50 μl of 0.5 mg/ml MTT solution in serum-free media was added. After 4 h of incubation, 150 μl of DMSO was added to dissolve the formazan crystals and the optical density was measured using a microplate reader at 570 nm. The results are expressed as the percentage of cell viability as compared to the control and the IC_{50} was determined using Graphpad prism 5 software (San Diego, CA, USA).

Statistical analysis. Data are represented as means±SD from three separate experiments. Statistical analysis was performed using two-way ANOVA with general linear model (Graph Pad Prism 5 software) followed by multiple comparison. A value of $p<0.05$ was considered statistically significant.

Results

Preparation of HA-decorated nanoparticles. PLGA-PEG-NH_2 conjugate formation was confirmed by ^{1}H NMR spectroscopy (data not shown). PLGA-PEG-NH_2 nanoparticles were prepared by O/W single-emulsion solvent evaporation method. HA was conjugated with free NH_2 groups of PEG *bis* amine protruding from nanoparticles by an EDC coupling reaction.

Characterization of nanoparticles. CTAB turbidimetric assay confirmed the presence of HA on nanoparticles. It was found that 0.116±0.031 mg (n=3) of HA was present per milligram of HA conjugated PLGA nanoparticles. Size, polydispersity and zeta potential of SN-38-loaded nanoparticles are summarized in Table I. The size of nanoparticles ranged from 245-270 nm with a polydispersity index of 0.139-0.155, and zeta potential was between -30 mV to -35 mV. As shown in Table I, encapsulation efficiencies of SN-38 in PLGA-PEG and PLGA-PEG-HA nanoparticles were 81.85±5.33 and 75.83±4.12% respectively.

CD44 receptor expression. CD44 expression levels were determined by flow cytometry. As shown in Figure 1, CHO cells exhibited very negligible expression, whereas ovarian cancer cell lines SKOV-3 and OVCAR-8 exhibited significantly high expression. Based on receptor expression, CHO cells were used as $CD44^-$ cells and SKOV-3 and OVCAR-8 cells were used as $CD44^+$ cells in further studies.

Specificity of HA-conjugated PLGA-PEG nanoparticles. To evaluate the cancer cell specificity of PLGA-PEG-HA nanoparticles, the cellular uptake of targeted nanoparticles loaded with FITC was tested in $CD44^-$ (CHO) and $CD44^+$ (SKOV-3 and OVCAR-8) cell lines and compared against the uptake of non-targeted nanoparticles (PLGA-PEG nanoparticles) using flow cytometry. Cells incubated only with cell growth medium without any nanoparticles were used as a negative control. Cellular uptake was tested at two concentrations of nanoparticles, 5 μg/ml and 25 μg/ml. The percent of cells showing internalized HA-decorated nanoparticles (as a function of fluorescence) was significantly higher in both cancer cell lines SKOV-3 and OVCAR-8, than in CHO (Figure 2). The difference was significant at 5 μg/ml ($p<0.001$) and at 25 μg/ml ($p<0.001$) of nanoparticles. Higher cellular fluorescence and percent of cells showing uptake of HA-conjugated PLGA-PEG nanoparticles in SKOV-3 and OVCAR-8 cells in comparison to CHO cells indicates greater specificity of PLGA-PEG-HA nanoparticles for ovarian cancer cells with higher CD44 expression levels. Since CD44 receptor expression was expressed as a percentage of cells expressing the CD44 receptor, not the receptor density, the difference in cellular uptake of nanoparticles between SKOV-3 and OVCAR-8 cells at 5 μg/ml is presumably due to a difference in receptor density. At higher concentration (25 μg/ml), irrespective of receptor density, almost 100% of these cells exhibited uptake.

To further examine the role of HA surface decoration in cellular internalization, uptake of targeted nanoparticles was also compared with that of non-targeted PLGA-PEG nanoparticles (Figure 2B). Surface decoration with HA did not increase cellular uptake in CHO cells, whereas in ovarian cancer cells, the uptake of the HA-decorated nanoparticles significantly increased in comparison to that of simple

PLGA-PEG nanoparticles. At both 5 and 25 μg/ml, ovarian cancer cells have shown higher uptake of HA-decorated nanoparticles.

Mechanism of cellular internalization. To evaluate the mechanism of cellular internalization, PLGA-PEG-HA nanoparticles were incubated with the endocytosis inhibitor colchicine. As shown in Figure 3, the presence of colchicine significantly reduced the internalization of the nanoparticles at both 5 μg/ml and 25 μg/ml concentrations ($p<0.05$). In order to test the involvement of CD44 receptor-mediated endocytosis, PLGA-PEG-HA nanoparticles were incubated with excess HA. The presence of HA also significantly reduced the cellular internalization of HA nanoparticles ($p<0.05$).

To further demonstrate the involvement of receptor-mediated endocytosis in nanoparticle uptake, the uptake of PLGA-PEG-HA nanoparticles was assessed at 4˚C and compared with their uptake at 37˚C. As shown in Figure 4, even at a high concentration of nanoparticles (25 μg/ml), negligible uptake was observed at 4˚C in both SKOV-3 and OVCAR-8, whereas at 37˚C, the uptake was >95% in both these cell lines.

Stability of SN-38-loaded nanoparticles. To determine the shelf-life of the lyophilized SN-38-loaded nanoparticles, the size of the nanoparticles was tested three months after their preparation. Nanoparticles were found to be easily re-dispersible and after reconstitution, the average size was 280.66±0.198 nm, which is slightly higher than their size immediately after their preparation, 265.6±3.82 nm. The colloidal stability of nanoparticles incubated in PBS was tested each day for three days. As shown in Figure 5B, there was only about a 4% increase in the size of nanoparticles after three days and polydispersity was also not significantly affected.

The goal of preparing tumor specific SN-38 nanoparticles is to deliver high quantities of SN-38 in its active lactone form to the tumor microenvironment. At a physiological pH of 7.4, SN-38 is hydrolyzed to its inactive lactone form. As SN-38-loaded nanoparticles are meant for parenteral administration, SN-38 release from the nanoparticles was determined for three days in PBS of pH 7.4 and FBS. All the samples were acidified before analysis for the complete conversion of SN-38 into its lactone form, considering all the released drug got converted to its inactive carboxylate form. As shown in Figure 5A, only 8.18±1.11% of SN-38 was released from nanoparticles upon incubation with PBS for three days, whereas, about 19.78±1.51% of SN-38 was released from nanoparticles in FBS, presumably due to interaction of the nanoparticles with FBS leading to aggregation and release of SN-38. However, since it is generally assumed that about 3-4 h are needed for complete biodistribution, the proposed nanoparticles may be considered stable for *in vivo* applications. Further studies to evaluate the *in vivo* efficacy of HA-decorated SN-38-loaded nanoparticles are in progress.

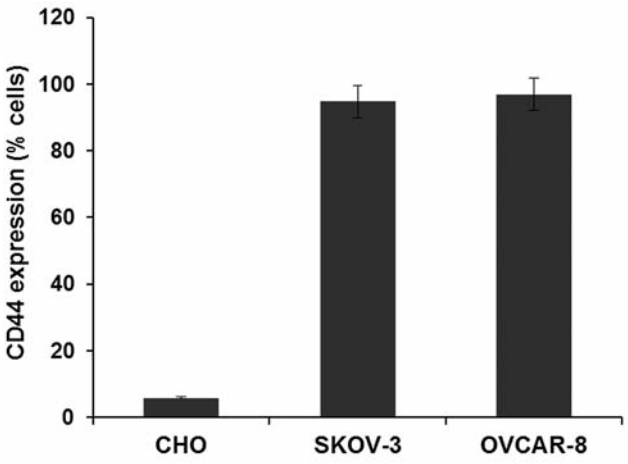

Figure 1. *CD44 receptor expression by flow cytometry. Cells (0.5×10^6) were incubated with FITC-labeled CD44 antibody at 4˚C for 30 min and the percentage of cells with fluorescence was measured by flow cytometry.*

In vitro cytotoxicity of nanoparticles. Finally, the cytotoxicity of SN-38-loaded PLGA-PEG and PLGA-PEG-HA nanoparticles was studied in OVCAR-8 and SKOV-3 cells. The IC_{50} values are shown in Figure 6. Targeted nanoparticles reduced cell viability in comparison to non-targeted nanoparticles and free drug in both the cell lines. In OVCAR-8 cells, IC_{50} values of SN-38 PLGA-PEG-HA NPs, SN-38 PLGA-PEG-NPs and free SN-38 were 229.9±7.65, 372.87±7.92, and 514.9±13.36 nM respectively ($p<0.05$). Whereas in SKOV-3 cells the IC_{50} values of SN-38 PLGA-PEG-HA NPs, SN-38 PLGA-PEG-NPs and free SN-38 were 6.21±0.14, 8.14±0.27, and 10.0±0.14 nM respectively ($p<0.01$).

Discussion

Poor solubility and poor stability of SN-38 compelled us to develop a PLGA nanoparticle system. Despite many advantages like small size, high payload, good stability and biocompatibility, clinical use of PLGA nanoparticles can be hampered by its rapid elimination from the circulation by reticuloendothelial system (RES). PEGylation of nanoparticles can significantly reduce its uptake by RES and increase their circulatory half-time (t½) (28). In this study a di-block copolymer PLGA-PEG was used to prepare PEGylated PLGA nanoparticles to reduce their recognition by RES. The specificity of these nanoparticles can be increased by the conjugation of a cancer targeting moiety on the surface of nanoparticles. Many cancer specific ligands

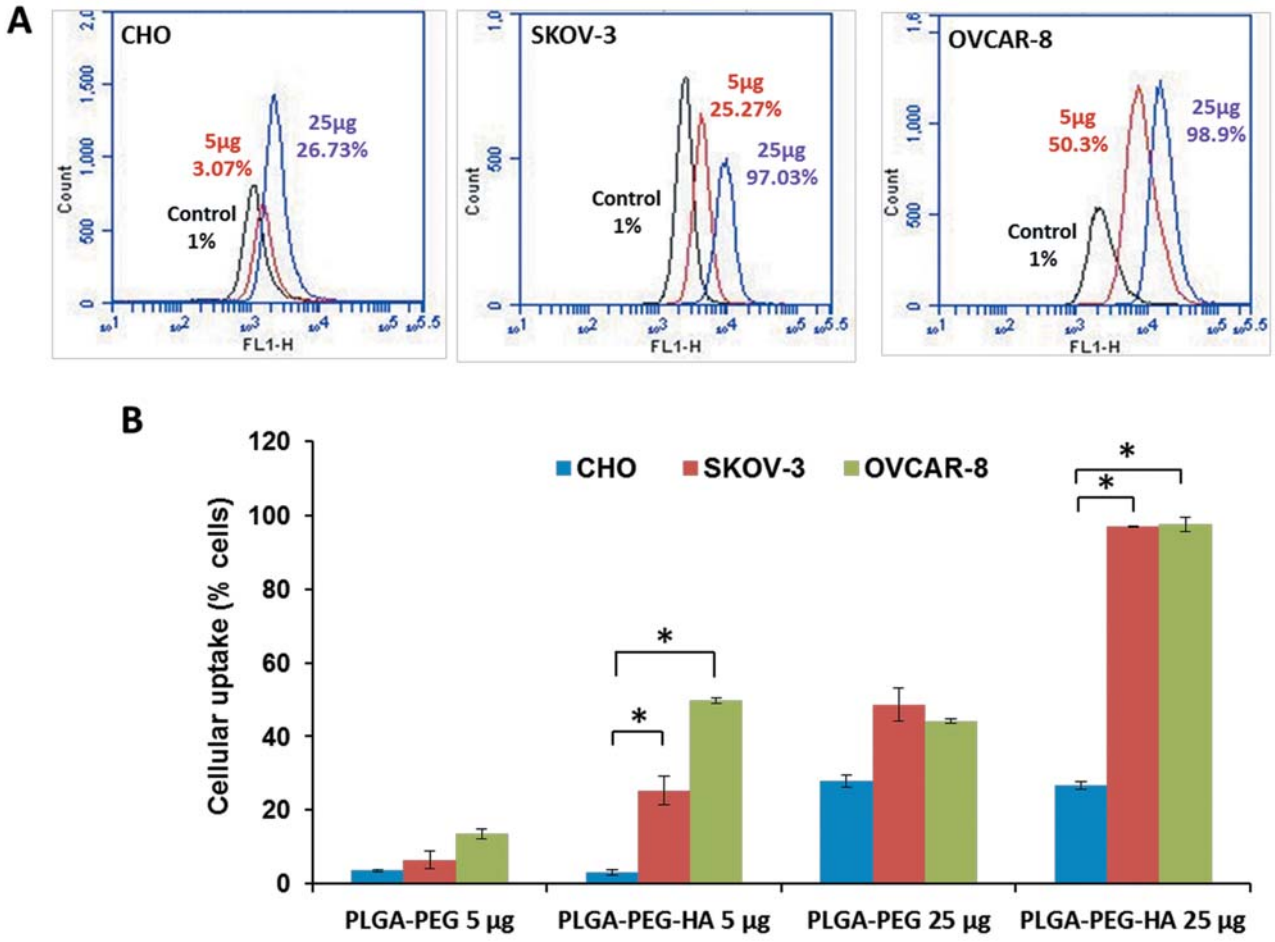

Figure 2. *Cellular uptake of targeted (HA-decorated PLGA-PEG) nanoparticles in comparison to that of non-targeted PLGA-PEG nanoparticles. A: Flow cytometric histograms displaying cellular uptake of PLGA-PEG-HA nanoparticles (as fluorescence intensity) at a concentration of 5 µg/ml (red curve) and 25 µg/ml (violet curve) compared to untreated cells (control, black curve) in CHO, SKOV-3 and OVCAR-8 cell lines. B: Percentage of cells showing uptake of PLGA-PEG-HA nanoparticles in comparison with PLGA-PEG nanoparticles at both concentrations 5 µg/ml and 25 µg/ml. Uptake of targeted nanoparticles is significantly greater in CD44$^+$ cells (SKOV-3 and OVCAR-8), in comparison with CD44$^-$ cells (CHO) at both concentration 5 µg/ml and 25 µg/ml (*$p<0.001$).*

have been used for targeted drug delivery of PLGA nanoiparticles (21, 29, 30). HA, a polysaccharide has been widely used as a cancer targeting moiety, due to its cancer specificity and biocompatibility. HA enters mammalian cells by endocytosis mediated by CD44 receptors which are highly expressed on various cancer cells. It is likely that any carrier system with HA as a targeting moiety can be internalized by cells through CD44-mediated endocytosis. Surface decoration of nanoparticles with HA significantly increased intracellular delivery of many chemotherapeutics in a target-specific manner (7).

The idea behind developing SN-38 encapsulated PLGA-PEG-HA nanoparticles is to deliver high amount of SN-38 specifically to cancer cells while circumventing the solubility problem and increasing hydrolytic stability of SN-38. In the present study, the surface decoration (conjugation of ligand onto the surface of nanoparticles) method was used to prepare HA-coated nanoparticles because PLGA-PEG-HA conjugate was not soluble in either organic solvents or water, which hampered the preparation of nanoparticles with PLGA-PEG-HA conjugate. Surface decoration has also been used to conjugate target-specific ligands such as polysaccharides (25) or peptides (31) onto nanoparticulate systems by an EDC coupling reaction.

According to Lesley *et al.* (32), HA with 6-18 sugars exhibited monovalent interaction with CD44 receptors, whereas HA with more than 22 sugars had a progressive increase in avidity towards CD44 receptors. This is due to the simple fact that HA with more saccharides can bind to more than one CD44 receptor. Interestingly, high molecular

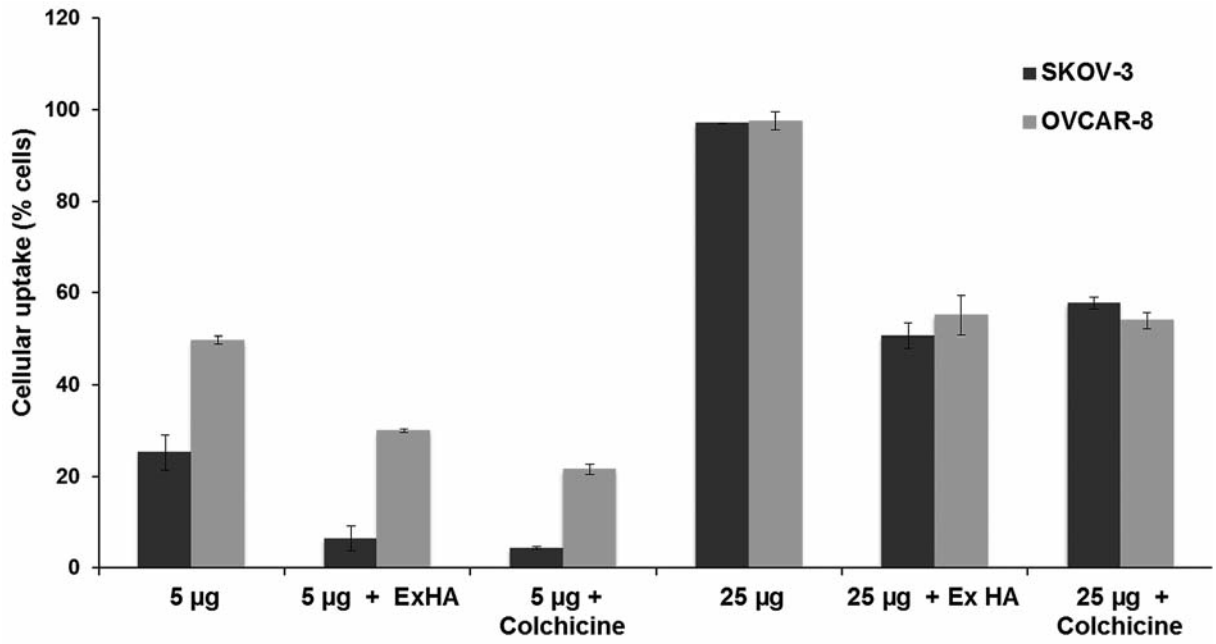

Figure 3. *Mechanism of internalization: Cellular uptake of hyaluronic acid (HA)-decorated (PLGA-PEG-HA) nanoparticles in presence of excess HA (1 mg/ml) or 20 µM colchicine. Cellular uptake of PLGA-PEG-HA nanoparticles was significantly reduced by the presence of colchicine and excess HA at both 5 µg/ml and 25 µg/ml nanoparticle concentrations ($p<0.05$).*

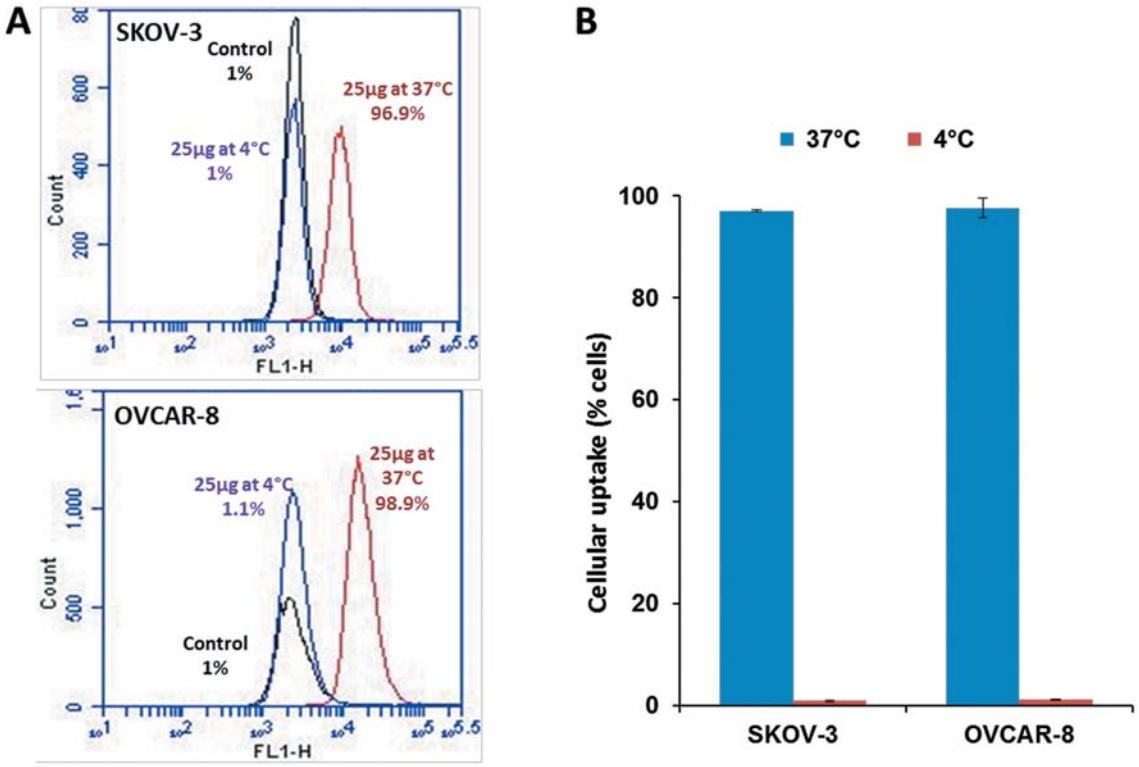

Figure 4. *Cellular uptake of PLGA-PEG-HA nanoparticles at 4˚C and 37˚C. A: Flow cytometric histograms displaying cellular uptake of PLGA-PEG-HA nanoparticles (25 µg/ml) at 4˚C (violet curve) and 37˚C (red curve) compared to untreated cells (control, black curve) in SKOV-3 and OVCAR-8 cell lines. B: The quantitative analysis of the percentage of cellular uptake (as fluorescence intensity) at 4˚C and 37˚C ($p<0.001$) in SKOV-3 and OVCAR-8 cells.*

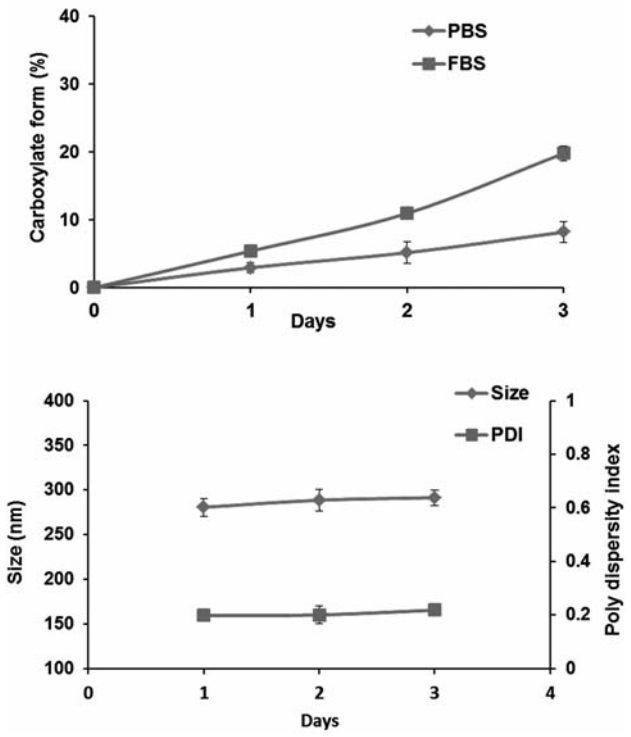

Figure 5. *A: Stability of SN-38 encapsulated in PLGA-PEG-HA nanoparticles showing the percentage of SN-38 in carboxylate form in pH 7.4 phosphate buffer saline (PBS) and fetal bovine serum (FBS). B: Colloidal stability of PLGA-PEG-HA nanoparticles. Average size and poly dispersity index of the nanoparticles dispersed in PBS are depicted.*

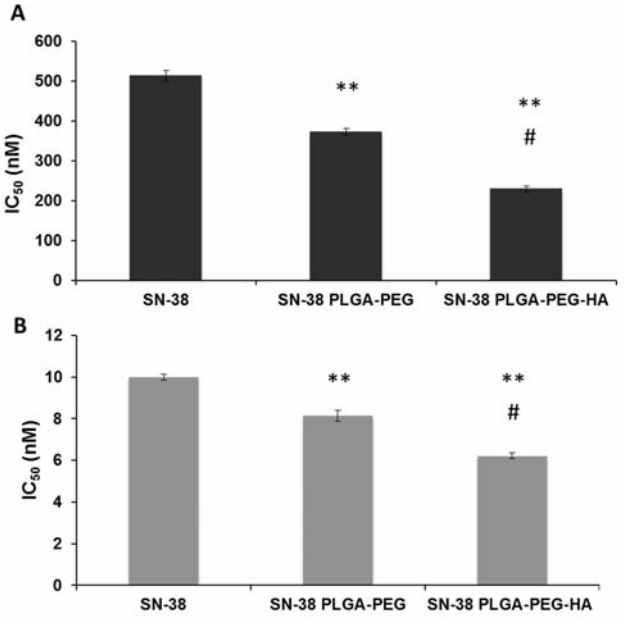

Figure 6. *Half-maximal inhibitory concentrations (IC_{50}) of SN-38, SN38-loaded PLGA-PEG nanoparticles, and SN38-loaded PLGA-PEG-HA nanoparticles for A: OVCAR-8 and B: SKOV-3 cell lines. **$p<0.005$ in comparison to SN-38, #$p<0.05$ in comparison to SN38 PLGA-PEG nanoparticles.*

weight HA (>200 kDa) had a short half-life *in vivo* and was cleared from circulation by HA receptor for endocytosis (HARE) present in liver and lung. Based on these results, a median size HA of about 40 saccharides (average Mw 16.9 kDa) was chosen for surface decoration of nanoparticles.

CTAB turbidimetric assay has been used to quantify the amount of HA. CTAB, which is chemically hexadecyl-trimmethylammonium bromide, is a cationic surfactant which binds to negatively charged polysaccharides, like HA ,to form insoluble complexes. The formation of these complexes is linear with the concentration of polysaccharides and can be used to quantify them (33). In the present study the amount of HA was quantified indirectly by the CTAB assay. It was found that HA was conjugated on to nanoparticles at 1:0.35 molar ratio (PLGA-PEG:HA).

Size and zeta potential of nanoparticles plays an important role in the stability of nanoparticles, their interaction with cell membrane and their *in vivo* fate (21). Nanoparticles used in this study showed a narrow size distribution with polydispersity of 0.139 to 0.155. Nanoparticles with higher zeta potential show greater colloidal stability in the suspension due to strong inter-particulate repulsive forces which prevent their aggregation. Nanoparticles used in this study possessed high zeta potential, >–30 mV. PLGA-PEG nanoparticles showed high encapsulation efficiency (81.85±5.33%) and further conjugation with HA did not significantly affect their encapsulation efficiency.

For the evaluation of cancer specificity, nanoparticles were loaded FITC, a hydrophobic fluorescent marker that makes it easy to encapsulate into hydrophobic PLGA nanoparticles. FITC-loaded nanoparticles (targeted and non-targeted) were incubated with cells for 30 min and analyzed for the percentage of cells showing fluorescence. The 30-min incubation period was selected based on studies conducted by Underhill *et al*. (34). They showed that binding of radiolabeled HA took place within 2 min of incubation, reached a maximum in 30 min and remained relatively constant for a period of 1 h. We, therefore, studied the uptake of the HA-decorated nanoparticles after 30 min incubation.

Flow cytometry studies revealed that the percentage of cells showing uptake of PLGA-PEG-HA nanoparticles (5 μg/ml) was 8- and 16- fold higher in $CD44^+$ ovarian cancer cells (SKOV-3 and OVCAR-8) as compared to $CD44^-$ CHO cells. The uptake of PLGA-PEG-HA nanoparticles was 2- to 3-fold higher than PLGA-PEG nanoparticles in $CD44^+$ cells, but no significant difference in their uptake was observed in $CD44^-$ cells. These results clearly indicate that enhanced uptake of nanoparticles by the ovarian cancer cells can be

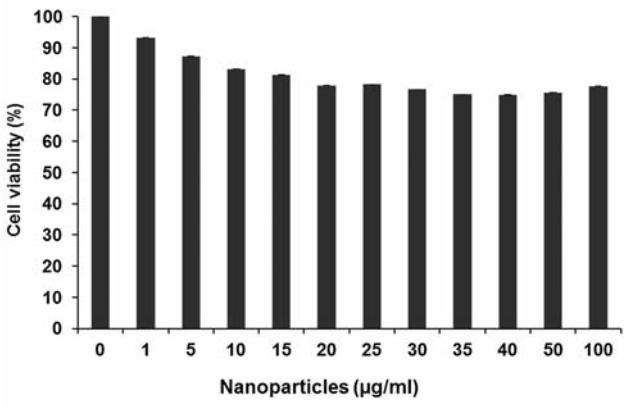

Figure 7. *In vitro toxicity of PLGA-PEG-HA nanoparticles to Chinese hamster ovary (CHO) cells.*

achieved by conjugating nanoparticles with HA. These results are consistent with previous studies in which HA was surface decorated on to nanoparticles to make them cancer specific and to enhance their cellular internalization (11, 18, 25, 35).

The mechanism of internalization of PLGA-PEG-HA nanoparticles was studied by incubating ovarian cancer cells with colchicine or excess HA. The presence of colchicine, an endocytosis inhibitor, significantly reduced the cellular uptake of PLGA-PEG-HA nanoparticles, indicating that endocytosis was involved in their uptake. The uptake of these nanoparticles was also decreased significantly in the presence of excess HA, indicating a competition for receptor binding between free HA and HA-decorated nanoparticles. These two experiments clearly indicate that PLGA-PEG-HA nanoparticles were internalized by CD44 receptor-mediated endocytosis.

To further probe the mechanism of internalization and to differentiate the surface adsorption of nanoparticles from endocytosis, the uptake study was conducted at two different temperatures 4˚C and 37˚C. As expected, the cellular uptake of PLGA-PEG-HA nanoparticles was negligible when incubated at 4˚C unlike at 37˚C, where it is significantly high. This could be possible due to the effect that active transport by receptor-mediated endocytosis is energy-dependent and therefore cannot occur at 4˚C (15). This experiment further substantiated that HA-decorated nanoparticles internalized through receptor-mediated endocytosis.

It is well-known that lyophilization with proper cryoprotectant can significantly increase the stability of nanoparticle formulation. In this study nanoparticles were lyophilized with 1% sucrose, which has been reported to maintain particle integrity after lyophilization of PLGA nanoparticles (36). PLGA-PEG-HA nanoparticles were easily re-dispersed and showed excellent colloidal stability in pH 7.4 PBS for three days. Encapsulation of SN-38 into nanoparticles significantly increased its hydrolytic stability in pH 7.4 PBS and FBS. There was only 20% of SN-38 released after 3 days incubation in FBS, retaining 80% of SN-38 inside nanoparticles in active lactone form.

Cytotoxicity of SN-38-loaded PLGA-PEG-HA nanoparticles was significantly higher than SN-38-loaded PLGA-PEG nanoparticles and free SN-38 presumably due to higher cellular internalization of the nanoparticles into the cancer cells. Another possible reason for increased cytotoxicity of the nanoparticles could be increased stability of SN-38. Nanoparticles act as intracellular drug depots and slowly release the SN-38 lactone form, which in turn enhances cytotoxicity (21). The toxicity study conducted on CHO cells (Figure 7), clearly shows that blank PLGA-PEG-HA nanoparticles (without SN-38) are non-toxic even at a concentration of 100 µg/ml. This is possible due to the fact that all the polymers (PLGA, PEG and HA) used in preparation of targeted nanoparticles were shown to be absolutely biocompatible.

To our knowledge, this is the first study on SN-38-loaded PLGA-PEG-HA nanoparticles for targeted ovarian cancer therapy. Physicochemical characteristics, targeting efficiency and cytotoxicity results from the present study demonstrate that the HA-decorated PLGA-PEG nanoparticles could be a better choice for targeted delivery of SN-38.

Disclosure

The Authors declare no conflicts of interest in this work.

Acknowledgements

This work was partially supported by a Texas A&M Health Science Center Cancer Research Council Seed Grant to SP.

References

1 Kalogera E, Dowdy SC, Mariani A, Aletti G, Bakkum-Gamez JN and Cliby WA: Utility of closed suction pelvic drains at time of large bowel resection for ovarian cancer. Gynecol Oncol *126*: 391-396, 2012.

2 Siegel R, Naishadham D, and Jemal A: Cancer statistics, 2013. CA Cancer J Clin *63*: 11-30, 2013.

3 Agarwal R and Kaye SB: Ovarian cancer: Strategies for overcoming resistance to chemotherapy. Nat Rev Cancer *3*: 502-516, 2003.

4 Palakurthi S, Yellepeddi VK and Vangara KK: Recent trends in cancer drug resistance reversal strategies using nanoparticles. Expert Opin Drug Deliv *9*: 287-301, 2012.

5 Yellepeddi VK, Kumar A, Maher DM, Chauhan SC, Vangara KK and Palakurthi S: Biotinylated PAMAM dendrimers for intracellular delivery of cisplatin to ovarian cancer: role of SMVT. Anticancer Res *31*: 897-906, 2011.

6 Yellepeddi VK, Kumar A and Palakurthi S: Biotinylated poly(amido)amine (PAMAM) dendrimers as carriers for drug delivery to ovarian cancer cells *in vitro*. Anticancer Res *29*: 2933-2943, 2009.

7 Ossipov DA: Nanostructured hyaluronic acid-based materials for active delivery to cancer. Expert Opin Drug Deliv *7*: 681-703, 2010.
8 Toole BP: Hyaluronan: from extracellular glue to pericellular cue. Nat Rev Cancer *4*: 528-539, 2004.
9 Orian-Rousseau V: CD44, a therapeutic target for metastasising tumours. Eur J Cancer *46*: 1271-1277, 2010.
10 Prud'homme GJ: Cancer stem cells and novel targets for antitumor strategies. Curr Pharm Des *18*: 2838-2849, 2012.
11 Ghosh SC, Neslihan Alpay S and Klostergaard J: CD44: a validated target for improved delivery of cancer therapeutics. Expert Opin Ther Targets *16*: 635-650, 2012.
12 Platt VM and Szoka FC Jr.: Anticancer therapeutics: targeting macromolecules and nanocarriers to hyaluronan or CD44, a hyaluronan receptor. Mol Pharm *5*: 474-486, 2008.
13 Toole BP, Wight TN and Tammi MI: Hyaluronan-cell interactions in cancer and vascular disease. J Biol Chem *277*: 4593-4596, 2002.
14 Nair HB, Huffman S, Veerapaneni P, Kirma NB, Binkley P, Perla RP, Evans DB and Tekmal RR: Hyaluronic acid-bound letrozole nanoparticles restore sensitivity to letrozole-resistant xenograft tumors in mice. J Nanosci Nanotechnol *11*: 3789-3799, 2011.
15 Eliaz RE and Szoka FC Jr.: Liposome-encapsulated doxorubicin targeted to CD44: A strategy to kill CD44-overexpressing tumor cells. Cancer Res *61*: 2592-2601, 2001.
16 Park K, Lee MY, Kim KS and Hahn SK: Target specific tumor treatment by VEGF siRNA complexed with reducible polyethyleneimine-hyaluronic acid conjugate. Biomaterials *31*: 5258-5265, 2010.
17 Danhier F, Ansorena E, Silva JM, Coco R, Le Breton A and Preat V: PLGA-based nanoparticles: an overview of biomedical applications. J Control Release *161*: 505-522, 2012.
18 Yadav AK, Mishra P, Mishra AK, Jain S and Agrawal GP: Development and characterization of hyaluronic acid-anchored PLGA nanoparticulate carriers of doxorubicin. Nanomedicine *3*: 246-257, 2007.
19 Yadav AK, Agarwal A, Rai G, Mishra P, Jain S, Mishra AK, Agrawal H and Agrawal GP: Development and characterization of hyaluronic acid decorated PLGA nanoparticles for delivery of 5-fluorouracil. Drug Deliv *17*: 561-572, 2010.
20 Zhao H, Rubio B, Sapra P, Wu D, Reddy P, Sai P, Martinez A, Gao Y, Lozanguiez Y, Longley C, Greenberger LM and Horak ID: Novel prodrugs of SN38 using multiarm poly(ethylene glycol) linkers. Bioconjug Chem *19*: 849-859, 2008.
21 Ebrahimnejad P, Dinarvand R, Sajadi A, Jaafari MR, Nomani AR, Azizi E, Rad-Malekshahi M and Atyabi F: Preparation and *in vitro* evaluation of actively targetable nanoparticles for SN-38 delivery against HT-29 cell lines. Nanomedicine *6*: 478-485, 2010.
22 Zhang JA, Xuan T, Parmar M, Ma L, Ugwu S, Ali S and Ahmad I: Development and characterization of a novel liposome-based formulation of SN-38. Int J Pharm *270*: 93-107, 2004.
23 Roger E, Lagarce F and Benoit JP: Development and characterization of a novel lipid nanocapsule formulation of Sn38 for oral administration. Eur J Pharm Biopharm *79*: 181-188, 2011.
24 Boddu SH, Jwala J, Chowdhury MR and Mitra AK: *In vitro* evaluation of a targeted and sustained release system for retinoblastoma cells using Doxorubicin as a model drug. J Ocul Pharmacol Ther *26*: 459-468, 2010.
25 Qhattal HS and Liu X: Characterization of CD44-mediated cancer cell uptake and intracellular distribution of hyaluronan-grafted liposomes. Mol Pharm *8*: 1233-1246, 2011.
26 Jwala J, Boddu SH, Shah S, Sirimulla S, Pal D and Mitra AK: Ocular sustained release nanoparticles containing stereoisomeric dipeptide prodrugs of acyclovir. J Ocul Pharmacol Ther *27*: 163-172, 2011.
27 Xuan T, Zhang JA and Ahmad I: HPLC method for determination of SN-38 content and SN-38 entrapment efficiency in a novel liposome-based formulation, LE-SN38. J Pharm Biomed Anal *41*: 582-588, 2006.
28 Jokerst JV, Lobovkina T, Zare RN and Gambhir SS: Nanoparticle PEGylation for imaging and therapy. Nanomedicine (Lond) *6*: 715-728, 2011.
29 Shen JM, Gao FY, Yin T, Zhang HX, Ma M, Yang YJ and Yue F: cRGD-functionalized polymeric magnetic nanoparticles as a dual-drug delivery system for safe targeted cancer therapy. Pharmacological research : the official journal of the Italian Pharmacological Society *70*: 102-115, 2013.
30 Sahoo SK and Labhasetwar V: Enhanced antiproliferative activity of transferrin-conjugated paclitaxel-loaded nanoparticles is mediated via sustained intracellular drug retention. Mol Pharm *2*: 373-383, 2005.
31 Sneh-Edri H, Likhtenshtein D and Stepensky D: Intracellular targeting of PLGA nanoparticles encapsulating antigenic peptide to the endoplasmic reticulum of dendritic cells and its effect on antigen cross-presentation *in vitro*. Mol Pharm *8*: 1266-1275, 2011.
32 Lesley J, Hascall VC, Tammi M and Hyman R: Hyaluronan binding by cell surface CD44. J Biol Chem *275*: 26967-26975, 2000.
33 Song J-M, Im J-H, Kang J-H and Kang D-J: A simple method for hyaluronic acid quantification in culture broth. Carbohydrate Polymers *78*: 633-634, 2009.
34 Underhill CB and Toole BP: Binding of hyaluronate to the surface of cultured cells. J Cell Biol *82*: 475-484, 1979.
35 Zaki NM, Nasti A and Tirelli N: Nanocarriers for cytoplasmic delivery: cellular uptake and intracellular fate of chitosan and hyaluronic acid-coated chitosan nanoparticles in a phagocytic cell model. Macromol Biosci *11*: 1747-1760, 2011.
36 Holzer M, Vogel V, Mantele W, Schwartz D, Haase W and Langer K: Physico-chemical characterisation of PLGA nanoparticles after freeze-drying and storage. Eur J Pharm Biopharm *72*: 428-437, 2009.

Received March 27, 2013
Revised April 24, 2013
Accepted April 25, 2013